

# Deformation Behavior of Weakly Segregated Block Copolymers. 1. Influence of Morphology of Poly(styrene-*b*-butyl methacrylate) Diblock Copolymers

R. Weidisch,<sup>\*,†</sup> M. Ensslen,<sup>‡</sup> G. H. Michler,<sup>‡</sup> and H. Fischer<sup>§</sup>

Max-Planck-Institut für Polymerforschung, Postfach 3148, D-55021 Mainz, Germany;  
Martin-Luther-Universität Halle-Wittenberg, Institut für Werkstoffwissenschaft,  
D-06099 Halle, Germany; and TNO Institute of Applied Physics, P.O. Box 595,  
Eindhoven, The Netherlands

Received February 9, 1999

**ABSTRACT:** The deformation behavior of poly(styrene-*b*-butyl methacrylate) diblock copolymers, PS-*b*-PBMA, is studied by high-voltage electron microscopy (HVEM) with in-situ deformation device and by TEM. This allows us to describe the craze growth and propagation in block copolymers with different morphologies. The influence of shape and orientation of morphology on deformation mechanism is discussed in correlation with tensile properties. For lamellar, hexagonal, and lamellar/hexagonal structures diversion of crazes and craze stopping mechanisms are observed. The discussion of the dependence of craze initiation stress,  $\sigma_c$ , on morphology is used to correlate the micromechanical deformation processes with tensile properties. In contrast to other block copolymers, it is shown that  $\sigma_c$  exceeds the value of pure PS at 76% PS due to the hexagonal morphology, high miscibility, and broadened interface of PS-*b*-PBMA which explains the improved tensile properties of weakly segregated block copolymers. It is shown that microphase separated morphologies, phase behavior, and interface formation have a pronounced influence on deformation behavior of PS-*b*-PBMA diblock copolymers.

## Introduction

It is well-known that the impact properties of homopolymers can be improved by the incorporation of a dispersed elastomeric phase. This effect is caused by multiple crazing or multiple cavitation with shear yielding.<sup>1,2</sup> Block copolymers generally show different deformation mechanisms compared to those of homopolymers, because the microphase separated morphologies in the nanometer scale are too small to initiate crazes.<sup>3</sup>

The crazes and the fibrils in block copolymers are thicker than observed in PS, which is attributed to the influence of the microphase separated structures in block copolymers.<sup>4</sup> Many authors have shown that for heterogeneous polymers such as HIPS and ABS a critical particle size exists. If the particle size become smaller than about 0.2  $\mu\text{m}$ , the size of the volume element in the region of stress concentration is smaller than the required value so that crazing does not occur.<sup>1,3</sup> The observation of a cavitation mechanism in block copolymers is in agreement with this critical particle size criterium. Schwier et al.<sup>5</sup> proposed a model for craze growth in block copolymers based on a mechanism of cavitation of the domains under the concentrated stresses of the craze tip, followed by drawing and fibril formation in the PS carcass. This is shown in Figure 1 where three rows of hexagonally packed cylinders are deformed by cavitation. The basic ingredients of this process are given in the tensile behavior of an idealized cube of material with ordered domains (spheres or hexagonally packed cylinder) in a matrix for example of PS. The material is then initially linearly

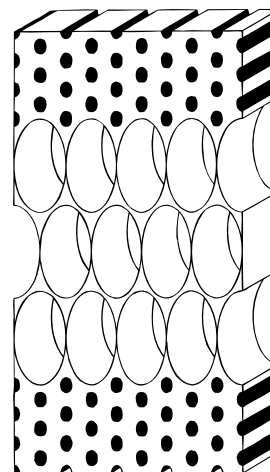


**Figure 1.** Model of cavitation mechanism in block copolymers with hexagonally packed cylinders suggested by Schwier et al.<sup>5</sup> for PS-*b*-PB diblock copolymers. The cavitation occurs in the PB rods followed by the plastic deformation of the PS matrix resulting in the craze structure.

elastic deformed up to a critical strain, where the domains cavitate under the concentrated stresses. The stress builds up in the surrounding matrix and can lead to a large plastic flow of the matrix and formation of fibrils under elevated stress. The formation of a stress field in the glassy matrix arising from the thermal stresses between the phases can be large in the case of PS-*b*-PB diblock copolymers due to the thermal mismatch of the expansion coefficient between PS and PB. Furthermore, the local stress concentration ahead of the craze tip also provides reasons for such elevated stress concentrations. The investigation of Argon and co-workers showed<sup>6</sup> that in PS-*b*-PB diblock copolymers a cavitation mechanism can be observed for different morphologies. Recently, Polis and Winey observed kink

\* To whom correspondence should be addressed.

<sup>†</sup> Max-Planck-Institut für Polymerforschung.

<sup>‡</sup> Institut für Werkstoffwissenschaft

<sup>§</sup> TNO Institute of Applied Physics.

**Table 1. Molecular Weight ( $M_n$ ), Volume Fraction ( $\Phi_{PS}$ ), and Polydispersity ( $M_w/M_n$ );  $\chi N$  Values at 120 °C ( $\chi = 0.0127$  at 120 °C [Ref 18]) and Morphology (TEM) for PS-*b*-PBMA Diblock Copolymers Used in This Study**

sample	$10^{-3}M_n^a$ copolymer ( $M_w/M_n$ )	PS <sup>b</sup> block	morphology (TEM)	$\chi N$
SBM 29	246.0 (1.04)	0.29	PS cylinder	24.33
SBM 50	278.0 (1.07)	0.51	lamellae (LAM)	29.50
SBM 55	534.0 (1.06)	0.55	lamellae	57.35
SBM 67	450.0 (1.05)	0.67	lamellae	50.10
SBM 70	286.0 (1.05)	0.70	lamellae	32.10
SBM 72	426.0 (1.04)	0.72	lamellae/PBMA cylinder (LAM/HEX)	48.10
SBM 74	463.0 (1.03)	0.74	LAM/HEX	52.60
SBM 76	459.0 (1.09)	0.76	PBMA cylinder (HEX)	52.40
SBM 83	383.1 (1.04)	0.83	PBMA spheres	44.60

<sup>a</sup> Size exclusion chromatography (SEC); values are based on the PS standards. <sup>b</sup> <sup>1</sup>H NMR.

band formation in poly(styrene-*b*-ethylene propylene) diblock copolymers by applying steady shear strain.<sup>7</sup> The deformation behavior of PS-*b*-PB-*b*-PS triblock copolymers, SBS, at higher strains has been intensively investigated by TEM, SAXS, and SANS.<sup>8–11</sup>

Russell et al.<sup>12,13</sup> reported data concerning the phase behavior of poly(styrene-*b*-butyl methacrylate), PS-*b*-PBMA, diblock copolymers. It was shown that PS-*b*-PBMA diblock copolymer melts show a microphase separation upon heating. These diblock copolymers exhibit both an upper critical order transition (UCOT) and a lower critical order transition (LCOT). Recently, Ruzette et al.<sup>14</sup> have shown that dPS-*b*-alkyl methacrylate diblock copolymers with long side chain methacrylates  $n \geq 6$  reveal an UCOT behavior. In contrast, diblock copolymers with short side chain methacrylates  $n < 5$  reveal a LCOT behavior.

In our previous studies<sup>15–18,33</sup> we reported morphologies, phase behavior, and tensile properties of the PS-*b*-PBMA diblock copolymer system depending on polystyrene content and molecular weight. It was shown that PS-*b*-PBMA diblock copolymers show synergistic effects on tensile properties mainly arising from their high miscibility and large interface width. In the present study the deformation mechanisms of PS-*b*-PBMA diblock copolymers at large strains depending on morphology will be presented.

## Experimental Section

**Sample Preparation.** All samples were dissolved in toluene. The solvent was allowed to evaporate slowly over 5–7 days at room temperature. Then the films were dried to constant weight in a vacuum oven at 120 °C for 3 days.

**Characterization.** The synthesis of PS-*b*-PBMA diblock copolymers was described previously by Arnold et al.<sup>15</sup> Measurements with size exclusion chromatography (SEC) were carried out using a Knauer-SEC with a RI/Viscodetector and a PS standard linear column. The volume fractions of the diblock copolymers were estimated by <sup>1</sup>H NMR. The molecular weights, compositions, and morphologies of the diblock copolymers used in this study are summarized in Table 1.

To investigate the micromechanical deformation behavior, semithin sections with a thickness on the order of 0.5  $\mu\text{m}$  were strained in a 1000 kV high-voltage electron microscope (HVEM, JEOL 1000) with an in-situ tensile device which gives the possibility to study the craze growth and propagation. The advantage of HVEM investigations is the possibility to use thicker sections (about 500–1000 nm) for closer comparison with bulk materials. To avoid a large decomposition of PBMA during in-situ deformation, the samples were also strained externally followed by the investigation in the HVEM. This

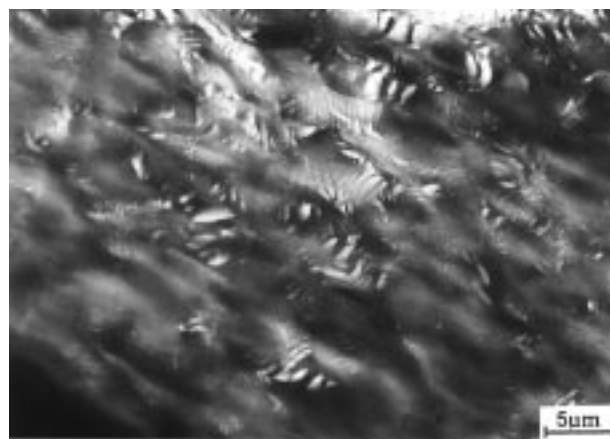


**Figure 2.** HVEM micrograph of deformation structure in sample SBM55 ( $\Phi_{PS} = 0.55$ ,  $M_n = 534$  kg/mol).

gives the possibility to look at a possible decomposition of PBMA in the electron beam. Furthermore, from deformed tensile bars with asymmetrical compositions ultrathin sections (50 nm) were cut at room temperature using glass knives in a Ultramicrotome (Reichert) for TEM investigations. The polystyrene blocks were stained with RuO<sub>4</sub> vapor. TEM investigations have been performed with JEOL 2000 FX (Eindhoven) and a BS500 (Halle) microscope.

## Experimental Results

To investigate the influence of morphology on deformation mechanism in block copolymers, PS-*b*-PBMA diblock copolymers with different compositions and  $M_n > 200$  kg/mol were used (Table 1). PS-*b*-PBMA diblock copolymers with PS contents lower than 39% PS reveal structures where a PBMA matrix is present. It was shown previously<sup>15</sup> that spherical and hexagonal structures exist in this composition range. These samples show a more homogeneous deformation of the PBMA matrix connected with a small tensile strength. The reason that for PS-*b*-PBMA diblock copolymers the tensile strength is generally higher than observed for PS-*b*-PB is that both components, PS and PBMA, are thermoplastic materials ( $T_{g,PBMA} = 31$  °C).<sup>16</sup> For block copolymers with lamellar structures at 50% PS a transition to a cavitation mechanism can be observed by HVEM. This is shown in Figure 2 for sample SBM55 with lamellar structures (534 kg/mol, 55% PS). It is obvious in the HVEM picture that the light PBMA lamellae are largely deformed often up to the extent of cavitation breakdown. This means that cavitation occurs in the PBMA phase. Once a critical value of stress concentration is achieved in the PBMA phase, a large-scale delamination and drawing occurs. The cavitation mechanism in this block copolymer is mainly localized to the PBMA phase and reveals a less distinct nature of the deformation zones as also observed by Argon<sup>19</sup> for triblock copolymers. In this sample macroscopic stress whitening is observed which is attributed to the large-scale delamination.

For block copolymers with 67% PS which also reveal a lamellar structure, a more localized cavitation mechanism can be observed, where the lamellae are stretched in the direction of applied stress. It is obvious in Figure 3 that narrow zones of highly deformed lamellae exist in this sample. These deformation zones propagate perpendicular to the direction of the applied stress which was also found for craze growth in homopolymers and blends. The crazes have a thickness up to 5  $\mu\text{m}$ ,

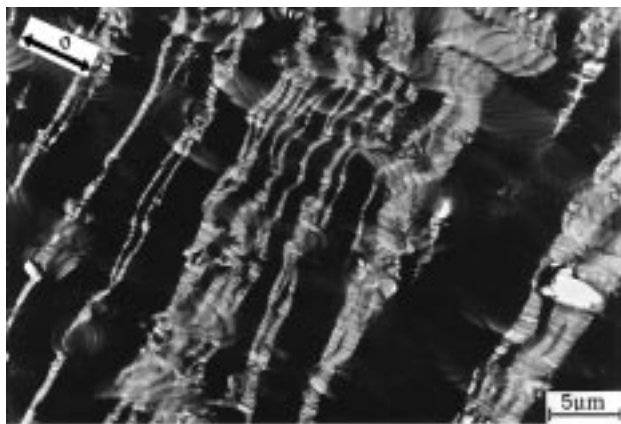


**Figure 3.** HVEM micrograph of crazes in a PS-*b*-PBMA diblock copolymer with lamellar structure (sample SBM67,  $\Phi_{PS} = 0.67$ ,  $M_n = 450$  kg/mol).

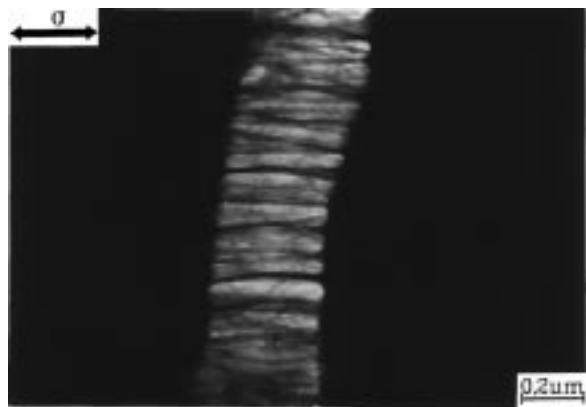


**Figure 4.** Higher magnification of a craze structure in a lamellar PS-*b*-PBMA diblock copolymer (SBM67  $\Phi_{PS} = 0.67$ ,  $M_n = 450$  kg/mol).

but many show a smaller thickness. This arises from the coalescence of thinner deformation zones into thick crazes. From micrographs with lower magnifications it was possible to determine their length. Typical values for the average length are 200–300  $\mu\text{m}$ . Comparing this with crazes observed in pure PS as shown by Koltisko et al.,<sup>20</sup> it appears that crazes in a 1600 kg/mol PS were typically large in number, but short, and randomly distributed. In contrast, PS-*b*-PBMA diblock copolymers with 67% PS (sample SBM67) exhibit fewer but much longer crazes. The same result was observed by Koltisko<sup>20</sup> for SBS triblock copolymers with spherical morphologies.

It is obvious in Figure 4 that the internal structure of the craze consists of highly deformed craze fibrils of PS and PBMA. The PS fibrils appear to be dark due to the larger thickness compared to the cavitated light PBMA. The light PBMA lamellae can easily cavitate due to their low modulus. As the stress concentration builds up at the PS lamellae the glass transition of PS is lowered due to applied stress field which leads to a large plastic deformation of the PS lamellae. This is the same mechanism as described by Argon for PS-*b*-PB diblock copolymers, typically called cavitation.<sup>5</sup> In contrast to PS-*b*-PB diblock copolymers, for PS-*b*-PBMA diblock copolymers the existence of asymmetrical phase compositions found by dynamic-mechanical analysis has a pronounced influence on the level of craze initiation stress.<sup>16</sup> From our results we concluded that an essentially pure PS matrix and a PS/PBMA mixed phase

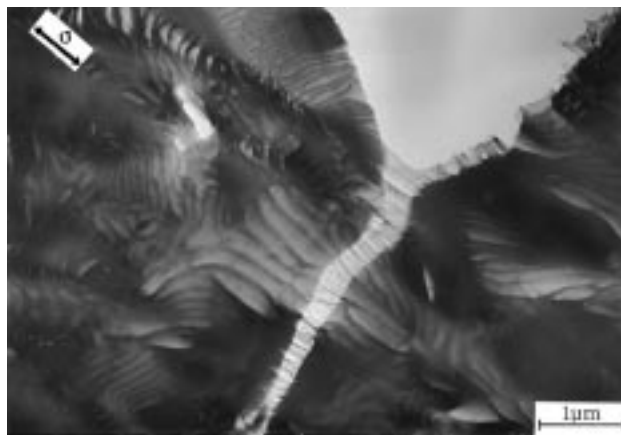


**Figure 5.** Lower magnification of a craze in a PS-*b*-PBMA diblock copolymer with lamellar morphology (SBM67,  $\Phi_{PS} = 0.67$ ,  $M_n = 450$  kg/mol).

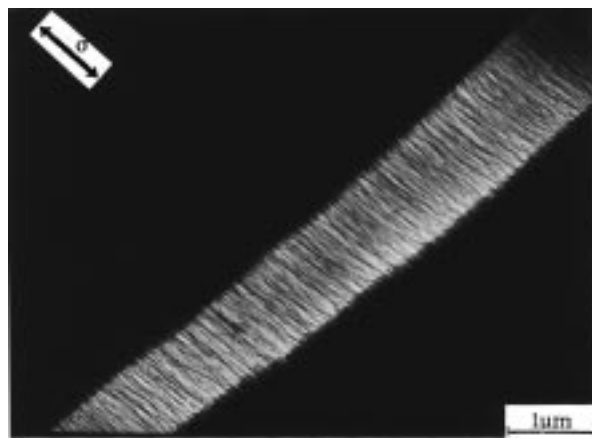


**Figure 6.** HVEM micrograph of craze structure in pure PS with  $M_n = 313$  kg/mol.

exist. The mixed phase increases the craze initiation stress,  $\sigma_c$ , compared to that of PS-*b*-PB, which then could be responsible for the improved tensile strength as discussed later. The PS fibrils in Figure 4 arise from highly deformed PS lamellae as clearly visible in Figure 5. The diameter of the PS fibrils is 15–25 nm, and the distance between the PS fibrils is about 100–130 nm. Figure 6 shows the microstructure of a craze in PS with a molecular weight of 313 kg/mol. Typical values for the thickness and distance between the fibrils are 2.5–10 nm and 10–50 nm, respectively. These values agree with data observed by other authors using different methods.<sup>21–23</sup> Comparing these values with the craze microstructure of sample SBM67 (67% PS) in Figures 4 and 5, it is obvious that the thickness of the PS fibrils as well as the distance between the fibrils is much larger than observed for unmodified PS. This means that the microstructure of crazes in lamellar PS-*b*-PBMA diblock copolymers arises from their microphase separated morphology. This confirms the results of Argon et al.<sup>5</sup> that the nucleation of crazes in block copolymers occurs via cavitation. From an TEM analysis of the undeformed morphology of sample SBM67 (67% PS), we obtained the thickness of the lamellae.<sup>15,16</sup> The observed values of 80–90 nm for the PS lamellae are much larger than observed for the thickness of the deformed PS lamellae. Therefore, the small thickness of the fibrils indicates a large plastic deformation. It was possible to determine the qualitative values for the extension ratio  $\lambda_{PS}$ . We can calculate a  $\lambda_{PS} = 5$ –6, which is higher than observed



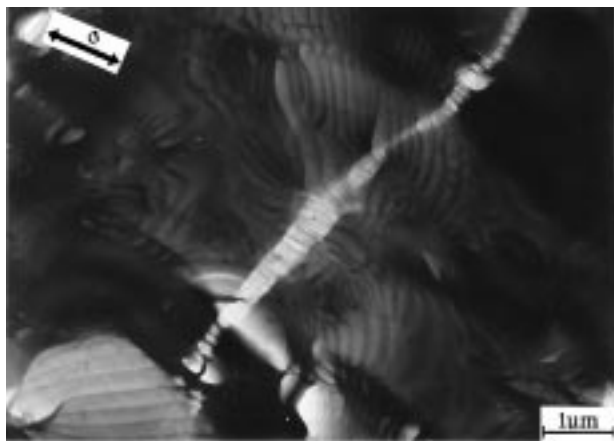


**Figure 7.** Influence of lamellar morphology of sample SBM67 ( $\Phi_{PS} = 0.67$ ,  $M_n = 450$  kg/mol) on craze propagation.

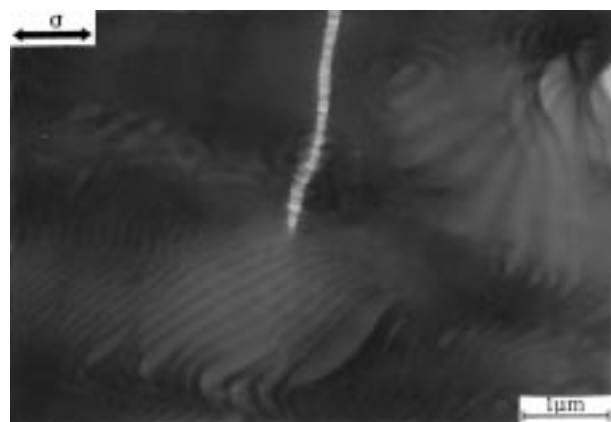


**Figure 8.** Mechanism of craze stop in a lamellar PS-*b*-PBMA diblock copolymer (SBM67  $\Phi_{PS} = 0.67$ ,  $M_n = 450$  kg/mol) causing improved strain at break due to energy dissipation. Also shown is the mature round craze tip which is sharp in the case of pure PS.

for PS ( $\lambda_{PS} = 4.3$ ).<sup>24</sup> The same results were observed by Creton et al.<sup>24</sup> for PS-*b*-PVP block copolymers which can be attributed to the stretched chain conformation in block copolymers.

An influence of morphology on craze growth and propagation is observed for lamellar structures. In Figure 7 diversion of crazes depending on the orientation of the morphology is shown. Normally, crazes propagate perpendicular to the direction of applied external stress field. This was also found for block copolymers with lamellar structures if the lamellae are oriented parallel to the stress field. If the lamellae are perpendicular or tilted toward to the applied stress, the deformation occurs in these lamellae (Figure 7). This means that craze propagation is influenced by the orientation of the lamellae and does not occur perpendicular to the external stress field in all cases. Furthermore, it was also found that stacks of lamellae were turned into the direction of stress applied due to rotation mechanism of the lamellae if the tilt angle between the lamellae and external stress direction is relatively small. Another observed mechanism is the termination of crazes at the borderline of stacks of lamellae (Figure 8). This is connected with a rounded craze tip of the stopped crazes. In pure PS the craze tip is typically sharp and well delineated, and the smallest resolvable voids near the tip are on the order of 10 nm.<sup>25</sup> In contrast, the craze tip shown in Figure 8 is less distinct

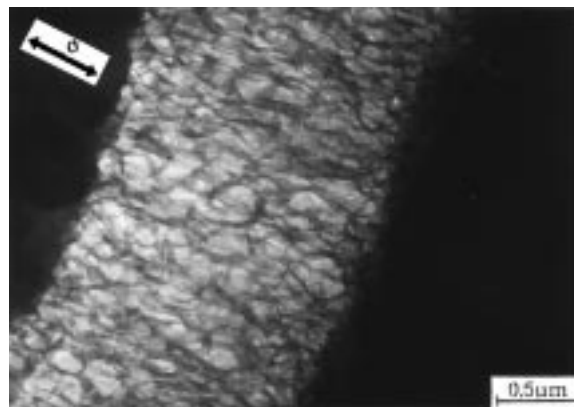


**Figure 9.** HVEM micrograph of craze structure of sample SBM76 ( $\Phi_{PS} = 0.76$ ,  $M_n = 459$  kg/mol) with hexagonally packed PBMA cylinders.



**Figure 10.** TEM micrograph of craze structure in a PS-*b*-PBMA diblock copolymer with hexagonal packed PBMA cylinders (SBM76,  $\Phi_{PS} = 0.76$ ,  $M_n = 459$  kg/mol); stained with  $\text{RuO}_4$ .

and not sharp. This is due to the observed craze termination mechanism and is clearly attributed to the influence of microphase separated structures on deformation mechanism. Stopping and diversion of crazes and the mature round craze tip cause higher strains at break due to the energy dissipation.

Figure 9 shows a HVEM picture of a craze in sample SBM 76 (76% PS). The cellular structure of the craze is quite similar to the model for the cavitation mechanism in block copolymers suggested by Argon<sup>5</sup> (shown in Figure 1). The light PBMA cylinders cavitate followed by a large plastic deformation of the dark PS matrix. The morphology is not shown in Figure 9 due to thickness of about 500 nm of the unstained films. The diameter of the PBMA cylinders is about 30–40 nm, which is much smaller than the thickness of the lamellae for samples discussed before. To discuss the influence of morphology on craze propagation, ultrathin sections were cut from external deformed tensile bars. As shown in Figure 10, the light PBMA cylinders are highly deformed and the PS matrix shows a large plastic deformation, indicating a cavitation mechanism as already observed in PS-*b*-PB diblock copolymers with

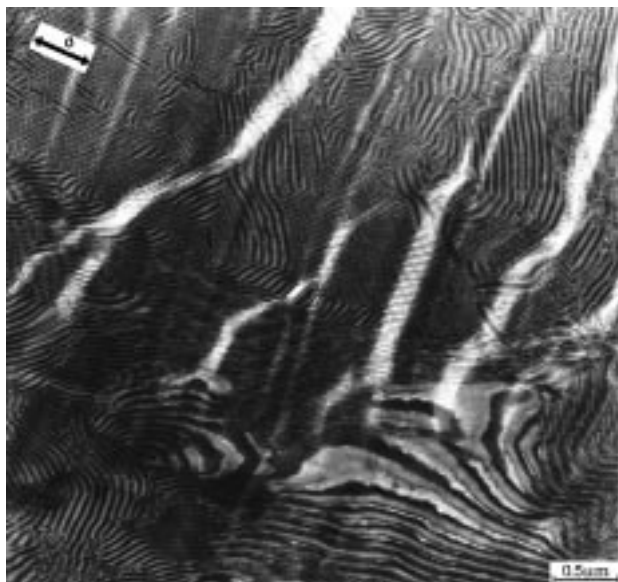


**Figure 11.** TEM micrograph of deformation structure in sample SBM72 revealing a coexistence of lamellae and hexagonally packed PBMA cylinders ( $\Phi_{PS} = 0.72$ ,  $M_n = 426$  kg/mol); stained with  $RuO_4$ .

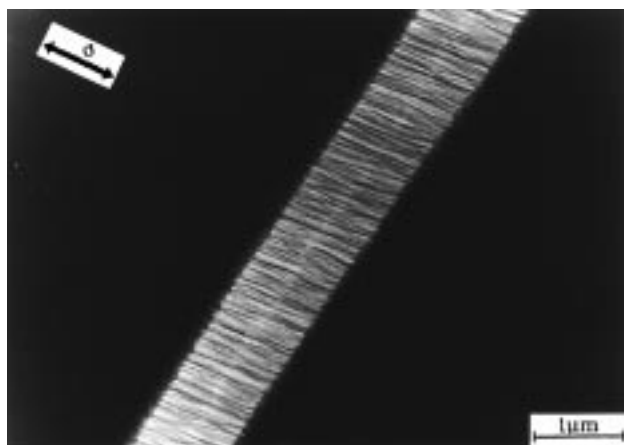


**Figure 12.** HVEM micrograph of a craze structure of sample SBM83 with PBMA spheres ( $\Phi_{PS} = 0.83$ ,  $M_n = 383$  kg/mol). At this composition a transition from cavitation to crazing can be observed.

cylindrical domains.<sup>5</sup> In contrast to this, diversion of crazes and craze stopping are observed for sample SBM72 (72% PS) which reveals a coexistence of lamellae and hexagonally packed cylinders.<sup>16,17</sup> It is obvious in Figure 11 that craze growth and propagation is strongly influenced by the direction of lamellar regions. If the lamellae are perpendicular to the craze direction, the crazes stopped at the borderline of these stacks. Furthermore, a diversion of crazes was found (Figure 11). This means that the observed deformation mechanisms appear to be a combination of both cylindrical and lamellar structures. For samples with spherical morphology at 83% PS (sample SBM83) the structures of the crazes are almost the same as observed for pure PS (Figure 12). This means that a transition from cavitation to crazing occurs which is in agreement with the results observed by Argon<sup>26</sup> in PS-*b*-PB diblock copolymers with about 5% PB.

### Discussion

Cavitation was observed in block copolymers with spherical, lamellar, and hexagonal morphologies,<sup>5,19,26</sup>

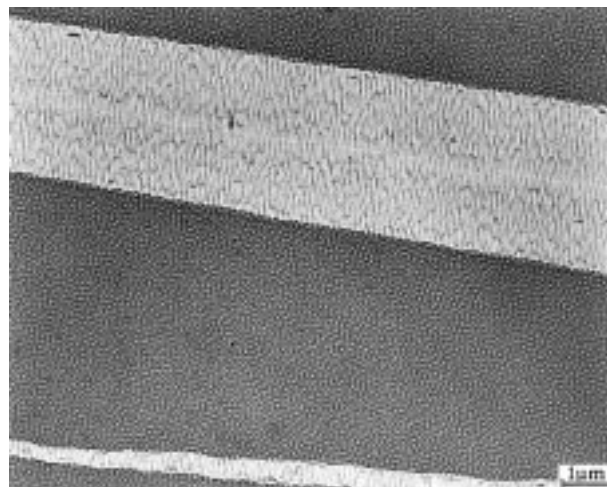


**Figure 13.** TEM micrograph of the initiate state of cavitation in a lamellar PS-*b*-PBMA diblock copolymer observed in a thin film (SBM67  $\Phi_{PS} = 0.67$ ,  $M_n = 450$  kg/mol).

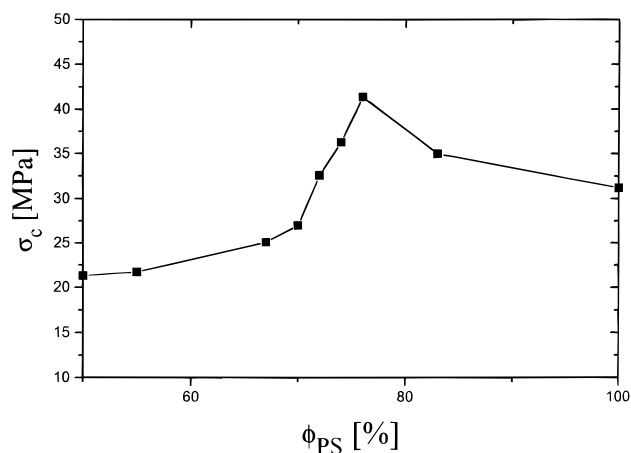


**Figure 14.** Dependence of craze initiation stress  $\sigma_c$  on volume fraction of PS for PS-*b*-PBMA diblock copolymers.

which leads us to the assumption that this mechanism also exists in PS-*b*-PBMA diblock copolymers. To confirm that craze growth in PS-*b*-PBMA diblock copolymers occurs via cavitation in Figure 13, the initial state of cavitation in sample SBM67 (67% PS) observed in a thin film (50 nm) is shown. It is obvious that both components show a large degree of plastic deformation arising from the deformation of the lamellar structure, which is clearly consistent with the picture of Argon et al.<sup>5</sup> The dark PS fibrils are highly deformed, which confirms the above-discussed cavitation mechanism. The cellular and network-like structure of the craze arises clearly from the microphase separated structure. The nonequilibrium morphology in Figure 13 differs from those of bulk equilibrium morphology due to the used small film thickness of about 50 nm.

To find out a correlation between deformation mechanism and mechanical properties, it is necessary to look at the influence of composition on craze initiation stress  $\sigma_c$ . In Figure 14,  $\sigma_c$  is plotted versus volume fraction of PS which shows the strong influence of morphology. It is surprising that  $\sigma_c$  increases in the composition range 60–80% PS and exceeds the value of pure PS. Koltisko et al.<sup>20</sup> observed a steep decrease of craze initiation stress for SBS triblock copolymers with 20–30% PB connected with a decrease of yield stress. In contrast, for PS-*b*-PBMA diblock copolymers a maximum of

tensile strength was found at 76% PS, which exceeds the value of pure PS of about 40%.<sup>17</sup> At this composition hexagonally packed PBMA cylinders were observed by TEM.<sup>17</sup> Recently, it was shown that the phase behavior of block copolymers can be correlated with their tensile properties.<sup>18</sup> Reasons for the synergistic effect on tensile strength of PS-*b*-PBMA are their large miscibility (intermediate segregation, see Table 1), the large interfacial width, and asymmetrical phase compositions.<sup>18</sup>

The craze initiation stresses,  $\sigma_c$  in Figure 14, are obtained from stress-strain curves where the curves deviate from their linear slope. Koltisko<sup>20</sup> obtained the craze initiation stress from the dependence of craze density on elongation. If one extrapolates this curve to zero craze density, one obtains the value of  $\sigma_c$ . We also tried to follow this way, but some problems arise from the exact determination of elongation during the in-situ experiments in HVEM. Furthermore, the exact values of the onset of the crazing process depend on the local value of elongation in the sample which could also lead to errors in the values observed by Koltisko et al.<sup>20</sup> Therefore, we compare  $\sigma_c$  of samples with LAM/HEX (72–74% PS) and HEX (76% PS) structures determined from stress-strain curves as well as from craze densities at different strains. In both cases the onset of crazing correlates with the onset of plastic deformation in the stress-strain diagram. Therefore, we used this criterion also for other compositions and the dependence of  $\sigma_c$  on composition shown in Figure 14 reflects the correlation between deformation microstructure and tensile properties. Our result leads to the conclusion that yielding is controlled by the deformation process (cavitation and nucleation of crazes).

It was shown by many authors that the interfacial strength in polymer blends is of great importance for the understanding of mechanical properties. Heikens et al.<sup>27</sup> have shown that the mechanical properties of poly(styrene)/poly(ethylene) blends can be improved by using SEBS block copolymers as interfacial compatibilizer.<sup>28</sup> The application of block copolymers led to a reduction of the interfacial energy which is combined with broadening of the interface. The reason for the improvement of mechanical properties is the enhancement of the interfacial strength between immiscible polymers. Kramer and co-workers<sup>29</sup> investigated the craze fracture at PS/PVP interfaces reinforced with PVP-*b*-PS-*b*-PVP triblock copolymers. It was shown that the energy release rate strongly depends on the block length of the used block copolymer, which means that the fracture toughness is strongly influenced by the interfacial width. From these results we could assume that in the case of PS-*b*-PBMA diblock copolymers the existence of an broadened interface is responsible for the improvement of tensile strength of PS-*b*-PBMA as compared to the case of PS-*b*-PB diblock copolymers with the same structure. For a symmetrical dPS-*b*-PBMA diblock copolymer with 248 kg/mol an interfacial width of 8.4 nm was observed by neutron reflectometry<sup>18</sup> due to their intermediate segregation (Table 1). As already discussed previously,<sup>17</sup> Bühler and Gronski<sup>31</sup> have shown for block copolymers that an increasing interface width leads to a decreasing interfacial energy. This is connected with a decreasing stress concentration at the interface which is responsible for the increase of craze initiation stress and tensile strength. This means that a reduction of critical stress concentration avoids a premature failure of the samples, and the craze initiation stress is larger

than in the case of strongly segregated block copolymers. Furthermore, the observed asymmetrical phase composition in PS-*b*-PBMA diblock copolymers also provides reasons for the enhanced values of  $\sigma_c$ . It was found by DMA<sup>15,16,33</sup> that an essential pure PS phase exists together with mixed PS/PBMA phase due to the asymmetrical phase diagram. For samples with HEX (76% PS) structure a PS matrix and a mixed PS/PBMA phase exist. While the PS matrix is responsible for the enhancement of strength of the matrix compared to the case of a PS/PBMA mixed phase, the mixed phase (cylinders) leads to an enhancement of critical cavitation stress. Because of the decreased stress concentration at the interface due to the broadened interfacial width, the craze initiation stress exceeds the value of pure PS for structures with a PS matrix.

This explains the measured maximum in tensile strength for HEX structures at 76% PS. For samples with 83% PS  $\sigma_c$  decreases because the deformation mechanism is changed to a pure crazing process. Therefore, a correlation between phase behavior, morphology, and craze initiation stress can be discussed. A maximum in craze initiation stress was not observed in the case of strongly segregated block copolymers such as PS-*b*-PB, where a strong decrease of  $\sigma_c$  as well as tensile strength was observed as the PB content increases.<sup>26</sup>

It was found by Creton et al.<sup>24</sup> that the extension ratio of the fibrils in PS-*b*-PVP block copolymers was always larger if the lamellae were oriented parallel to the craze fibril direction than if the lamellae were oriented perpendicular to this direction. This observation was attributed to the stretched chain conformation in block copolymers normal to the interfaces of the lamellae. Further, in both directions the values of extension ratio  $\lambda$  were larger than measured for the homopolymers PS and PVP. Also, for PS-*b*-PBMA diblock copolymers the observed values of  $\lambda_{PS}$  are higher than for pure PS arising from the stretched chain conformation. It was shown elsewhere<sup>32</sup> that a prestretching of PS leads to a strong increase of  $\lambda$ , which has led to the conclusion that a stretched chain conformation in block copolymers has a pronounced influence on extension ratio of the fibrils.

It was shown for different compositions that the microphase separated morphologies have a pronounced influence on craze propagation. The observed mechanisms of diversion and stopping of crazes can be discussed as reasons for the relatively high strain at break of about 40% for sample SBM67 (67% PS, lamellae). PS-*b*-PB diblock copolymers with lamellar structures are quite brittle due to small strength of the PB lamellae. For example, PMMA-*b*-PBMA diblock copolymers with nearly symmetrical compositions reveal a strain at break of only 20%.<sup>18</sup> (For a symmetrical PS-*b*-PBMA diblock copolymer the strain at break is about 50%.<sup>17</sup>) The reason for this different strains at break is the smaller miscibility of PMMA-*b*-PBMA diblock copolymers compared to that of PS-*b*-PBMA.<sup>18</sup>

For samples with LAM/HEX (72% PS) and HEX (76% PS) structures different deformation mechanisms are observed. While the propagation of crazes in samples with 76% PS mainly depends on the orientations of the cylinders, in samples with 72% PS also the regions of lamellae influence the direction of craze growth as shown in Figures 10 and 11. For samples with HEX structures (76% PS) the crazes propagate preferentially



through regions where the cylinder axes are transversely oriented to the external applied stress direction. This was already found by Schwier et al.<sup>5</sup> for PS-*b*-PB diblock copolymers with about 25% PB. In contrast, for samples with LAM/HEX structures (72–74% PS) the grains of lamellae lead to a diversion of crazes and craze stopping as already discussed for samples with pure lamellar structures. This causes a higher strain at break for samples with LAM/HEX structures as compared to samples revealing a pure HEX (76% PS) structure. This explains that a transition from brittle to more tough behavior can be observed as the content of PS decreases from 76% to 74%.<sup>17</sup> The strain at break increases from 4% for sample SBM76 (76% PS) up to 14% for SBM72 (72% PS). For samples with PBMA spheres (samples SBM83, 83% PS) it was shown elsewhere<sup>16</sup> that the tensile properties are almost the same as pure PS, which is in agreement with the observed transition from cavitation to crazing shown in Figure 12.

For strongly segregated block copolymers the interfacial width is much smaller than observed for PS-*b*-PBMA so that the stress transfer across the interface is not so effective, and a premature failure at a smaller strength and strain occurs especially for lamellar structures. Schnell et al.<sup>34</sup> have shown that for different blends the fracture toughness is correlated with the interfacial width. A transition from chain pullout to crazing was observed using the asymmetric double cantilever beam method as the interface increased up to about 6–11 nm. The mechanism of chain scission inside the plastic zone becomes the increasingly dominant failure mechanism with increasing interfacial width and the fracture toughness of the interface increases.<sup>34</sup> For an enhanced fracture toughness, a distinct degree of interpenetration of chains lower than the average distance between the entanglement points (9.3 nm for PS) is necessary in the interfacial region so that a significant portion of the strands may be loops rather than chain ends and an equivalent stress can be sustained by the interface with a much shorter interpenetration distance. In block copolymers, the chains are chemically coupled in the interfacial region, and a chain pullout therefore does not occur. The interfacial width of PS-*b*-PBMA diblock copolymers is in the same order where Schnell et al.<sup>34</sup> have found the strong influence of interfacial width on fracture toughness of the interface. The increase of the interfacial width enables an interpenetration of chains in the interfacial region which then can sustain a higher stress. If the stress is high enough, a large plastic zone will form, and a large energy dissipation can occur in the interfacial region. Therefore, deformation mechanisms such as diversion and stopping of crazes are more effectively than in strongly segregated block copolymers because of the large energy dissipation in the interfacial region. These processes are responsible for the enhanced toughness of lamellar and hexagonal structures compared to the case of block copolymers, revealing a lower miscibility such as PMMA-*b*-PBMA.<sup>18</sup>

While the phase behavior and interface formation of weakly segregated block copolymers provide reasons for their improved tensile properties, the discussion of the influence of morphology and phase behavior on deformation mechanisms is necessary to understand the correlation between deformation mechanisms and tensile properties.

It is shown that the transition to localized deformation zones occurs at a polystyrene content of 67% for lamellar structures, where the strain at break decreases from 55% to 40%. With increasing PS content up to 72% a LAM/HEX structure is present. It was already discussed that the combination of deformation mechanisms of pure lamellar and hexagonal structure is responsible for the improved strain at break compared to the HEX structure at 76% PS. For pure HEX structure the change of deformation mechanism is responsible for the observed tough to brittle transition at 76% PS. For hexagonal structures the crazes preferentially propagate through regions with transversely oriented cylinders, and in LAM/HEX structures mechanisms of diversion and termination of crazes are observed at the grain boundary of the lamellae which cannot be observed in pure HEX structures. In contrast to LAM and LAM/HEX structures a PS matrix is present for the HEX structure which is responsible for the observed maximum in craze initiation stress at 76%. For spherical structure at 83% PS the change of deformation mechanism from cavitation to crazing is responsible for the strong decrease in tensile strength, strain at break, and craze initiation stress. The observed deformation mechanisms can be also discussed in correlation with local orientation and grain boundaries of the microphase separated morphology in block copolymers. While a change in local orientation of the morphology leads to mechanisms such as diversion of crazes and rotation of lamellae (Figure 7), grain boundaries in different morphologies are responsible for the process of termination of crazes shown in Figures 8 and 11 for LAM and LAM/HEX structures.

This means that both the microphase separated morphologies and phase behavior (miscibility and interface formation) have a pronounced influence on deformation mechanisms (craze growth and initiation) of weakly segregated block copolymers. Only if we discuss both influences is it possible to understand the correlation between morphology, deformation mechanisms, and tensile properties of weakly segregated block copolymers.

## Conclusions

In the present study the deformation mechanisms of PS-*b*-PBMA diblock copolymers are investigated as an example for weakly segregated block copolymers. For samples with lamellar structures at 67% PS a transition to localized deformation zones is found. Furthermore, for lamellar structures mechanisms of diversion and termination of crazes are associated with a relatively high strain at break. Samples with LAM/HEX structures reveal a combination of deformation mechanisms of pure HEX and LAM structure, which is responsible for their enhanced toughness. The existence of a PS matrix at 76% PS is associated with a maximum in tensile strength. For samples with PBMA spheres at a PS content of 83% a transition from cavitation to crazing occurs, which explains the brittle property of these block copolymers.<sup>16</sup>

The observed large extension ratios for PS fibrils show clearly that the stretched chain conformation in block copolymers have a strong influence on properties of block copolymers. The strong increase of craze initiation stress for PS-*b*-PBMA block copolymers with 60–80% PS, which exceeds the value of pure PS, is in contrast to the previous observation in SBS triblock copolymers.

In contrast to strongly segregated block copolymers the increased interfacial width of weakly segregated block copolymers is responsible for the observed maximum in craze initiation stress at 76% PS.

It is demonstrated that the shapes of microphase separated morphologies as well as phase behavior and interface formation have a pronounced influence on deformation mechanisms (craze growth and craze initiation) of weakly segregated block copolymers. The investigation of deformation mechanisms led to a better understanding of the improved tensile properties of weakly segregated block copolymers.

**Acknowledgment.** The authors thank Mrs. E. Horig (Halle) for the TEM investigations of some of the diblock copolymers. R.W. acknowledges postdoctoral support (MPI Mainz) from Deutsche Forschungsgemeinschaft (DFG). We also acknowledge the helpful discussions with Dr. V. Abetz (Bayreuth) and Prof. V. Altstadt (Hamburg) and the synthesis of the used block copolymers in the groups of Doz. Dr. M. Arnold (Halle, Germany) and Prof. R. Jerome (Liege, Belgium). This work was supported in part by the Landesprojekt Sachsen-Anhalt "Neue Funktionswerkstoffe auf der Grundlage schwach entmischter Blockcopolymeren".

## References and Notes

- (1) Bucknall, C. B. *Toughened Plastics*; Appl. Sci. Publ. Ltd.: London, 1977.
- (2) Michler, G. H. *Kunststoffmikromechanik*; Carl Hanser Verlag: München, 1992.
- (3) Argon, A. S.; Cohen, R. E. In *Crazing in Polymers*; Kausch, H. H., Ed.; Springer-Verlag: Berlin, 1983; Vol. 1.
- (4) Argon, A. S. *Pure Appl. Chem.* **1975**, *43*, 247.
- (5) Schwier, C. E.; Argon, A. S.; Cohen, R. E. *Polymer* **1985**, *26*, 1985.
- (6) Argon, A. S.; Cohen, R. E. In *Crazing in Polymers*; Kausch, H. H., Ed.; Springer-Verlag: Berlin, 1990; Vol. 1.
- (7) Polis, D. L.; Winey, K. *Macromolecules* **1998**, *31*, 3617.
- (8) Segula, R.; Prud'homme, J. *Macromolecules* **1985**, *18*, 1295.
- (9) Odell, J. A.; Keller, A. *Polym. Eng. Sci.* **1977**, *17*, 544.
- (10) Pakula, T.; Saijo, K.; Kawai, H.; Hashimoto, T. *Macromolecules* **1985**, *18*, 1295.
- (11) Sakamoto, J.; Sakurai, S.; Doi, K.; Nomura, S. *Macromolecules* **1993**, *26*, 3351.
- (12) Russell, T. P.; Karis, T. E.; Gallot, Y.; Mayes, A. M. *Nature* **1994**, *368*, 729.
- (13) Karis, T. E.; Russell, T. P.; Gallot, Y.; Mayes, A. M. *Macromolecules* **1995**, *28*, 1129.
- (14) Ruzette, A.; Banerjee, P.; Mayes, A. M.; Pollard, M.; Russell, T. P.; Jerome, R.; Slawicki, T.; Hjelm, R.; Thiagarajan, P. *Macromolecules* **1998**, *31*, 8509.
- (15) Arnold, M.; Hofmann, S.; Weidisch, R.; Neubauer, A.; Poser, S.; Michler, G. H. *Macromol. Chem. Phys.* **1998**, *199*, 1, 31.
- (16) Weidisch, R.; Michler, G. H.; Fischer, H.; Hofmann, S.; Arnold, M.; Stamm, M. *Polymer* **1999**, *40*, 1191.
- (17) Weidisch, R.; Stamm, M.; Michler, G. H.; Fischer, H.; Jerome, R. *Macromolecules* **1999**, *32*, 742.
- (18) Weidisch, R.; Stamm, M.; Schubert, D. W.; Arnold, M.; Budde, H.; Höring, S. *Macromolecules* **1999**, *32*, 3405.
- (19) Argon, A. S.; Cohen, R. E.; Jang, B. Z.; Vandersande, J. B. *J. Polym. Sci., Polym. Phys. Ed.* **1981**, *19*, 253.
- (20) Koltisko, B.; Hiltner, A.; Baer, E. *J. Polym. Sci., Polym. Phys.* **1986**, *24*, 2167.
- (21) Michler, G. H. *Ultramicroscopy* **1984**, *15*, 81.
- (22) Beahan, P.; Bevis, M.; Hull, D. J. *Mater. Sci.* **1973**, *8*, 162.
- (23) Donald, A. M.; Chan, T.; Kramer, E. J. *J. Mater. Sci.* **1981**, *16*, 669.
- (24) Creton, C.; Kramer, E. J.; Hadziioannou, G. *Macromolecules* **1991**, *24*, 1846.
- (25) Zhurkov, S. N.; Kuksenko, V. S.; Slutsker, A. I. In *Fracture*; Chapman and Hall: New York, 1969.
- (26) Schwier, C. E.; Argon, A. S.; Cohen, R. E. *Philos. Mag.*, A **1985**, *52*, 5, 581.
- (27) Heikens, D.; Hoen, N.; Barentsen, W.; Piet, P.; Ladan, H. *J. Polym. Sci., Polym. Symp.* **1978**, *62*, 309.
- (28) Legge, N. R.; Holden, G.; Schroeder, H. E. *Thermoplastic Elastomers. A Comprehensive Review*; Hanser: Munich, 1987.
- (29) Washiyama, J.; Creton, C.; Kramer, E. J.; Xiao, F.; Hui, C. Y. *Macromolecules* **1993**, *26*, 6011.
- (30) Schubert, D. W.; Weidisch, R.; Stamm, M.; Michler, G. H. *Macromolecules* **1998**, *31*, 3743.
- (31) Bühler, F.; Gronski, W. *Makromol. Chem.* **1987**, *188*, 2995.
- (32) Maestrini, C.; Kramer, E. J. *Polymer* **1991**, *32*, 609.
- (33) Fischer, H.; Weidisch, R.; Stamm, M.; Michler, G. H.; Arnold, M., submitted for publication in *Macromolecules*.
- (34) Schnell, R.; Stamm, M.; Creton, C. *Macromolecules* **1999**, *32*, 3420.

MA9901801